Teknomekanik, Vol. 9, No. 2, 2026, pp. 238-255
e-ISSN: 2621-8720 p-ISSN: 2621-9980

Performance evaluation of a standalone PCA-based denoising method for Distributed Acoustic Sensing (DAS) data

Monowar Mahmud[1], Aiman Ismail[1,2*], Fairuz Abdullah[1,2], Hui Jing Lee[1,3], Nur Luqman Saleh[4], Abdul Hadi Sulaiman[5]

[1] Department of Electrical and Electronic Engineering, Universiti Tenaga Nasional, **Malaysia**
[2] Institute of Power Engineering, Universiti Tenaga Nasional, **Malaysia**
[3] Institute of Sustainable Energy, Universiti Tenaga Nasional, **Malaysia**
[4] Department of Computer and Communications System Engineering, Faculty of Engineering, Universiti Putra Malaysia, **Malaysia**
[5] School of Physics, Universiti Sains Malaysia, **Malaysia**

*Corresponding Author: aiman@uniten.edu.my
Received: 22 August 2025; *Revised:* 14 January 2026; *Accepted:* 18 January 2026

Cite this https://doi.org/10.24036/teknomekanik.v9i2.44372

Abstract: This paper experimentally evaluates the effectiveness of Principal Component Analysis (PCA) for denoising distributed acoustic sensing (DAS) data. Experiments were conducted by applying different vibration strengths using a piezo-electric transducer (PZT) at various sensing locations along the sensing fiber. Unlike existing hybrid PCA-based DAS denoising approaches, this work explicitly investigates PCA as a standalone denoising framework, addressing the lack of systematic evaluation of its effectiveness and practical applicability. Results show that PCA improves the signal-to-noise ratio (SNR) by at least 4.7 dB across a range of strain levels. The SNR also shows improvements exceeding 5 dB for sensing fiber lengths up to ~5.2 km. For ~10.2 km vibration location, PCA still achieved around 2.45 dB of SNR improvement. The PCA algorithm was then compared with traditional denoising algorithms, i.e., Moving Average, Low-Pass Filtering, and Wavelet Denoising, at a fixed sensing fiber length of 3.2 km and 2 Vpp applied to the PZT. PCA outperformed these approaches in noise reduction while maintaining moderate computational cost. Overall, PCA effectively suppresses background noise while preserving the integrity of the vibration signal. These results indicate that standalone PCA is a practical denoising option for DAS applications that require improved SNR at a moderate processing cost.

Keywords: denoising algorithm; distributed acoustic sensing; PCA performance; principal component analysis

1. Introduction

Distributed acoustic sensing (DAS) based on phase-sensitive optical time domain reflectometry (ϕ-OTDR) continuously monitors externally imposed vibrations on the optical fiber [1]. It provides unparalleled spatial resolution and temporal sampling rates for detecting and analyzing seismic and acoustic signals [2]. Currently, DAS has been applied in various fields, including seismic activity detection [3], [4], [5], [6], infrastructure health monitoring [7], pipeline leak detection [8], [9], [10], [11], [12], [13], [14], vehicle monitoring [15], and surveillance systems [16], [17], [18], [19], [20], etc.

DAS signals may be negatively affected by various types of noise. The primary contributors include thermal noise in the optical fibers will vary based on temperature-dependent environmental changes [21], shot noise at lower optical power levels [22], laser phase noise, or fluctuation of the phases of the source laser [23] and Rayleigh noise, which comes from random fluctuating backscattered

light that introduces uncertainty into the measurements, resulting in a reduction of the system's possible spatial resolution due to the uncertainty introduced into the measurements [24].

These noises significantly impact system performance by reducing the signal-to-noise ratio (SNR), masking weak signals, and creating spike-like artifacts in the raw data that can lead to false positives. They also distort essential signal features such as amplitude, phase, and frequency, degrading spatial resolution and making it difficult to localize vibrations accurately along the fiber. High noise levels reduce the system's sensitivity to low-level vibrations, impairing its ability to detect subtle environmental changes and causing errors in identifying vibration sources or types. This leads to unreliable measurements, increased false alarms, and diminished effectiveness in seismic monitoring, pipeline leak detection, and surveillance [25].

Therefore, it is essential to reduce noise levels in acquired DAS signals. Researchers in recent studies have proposed hardware-based noise improvement techniques, such as low-noise laser sources [26], enhanced backscattering fiber [27], or high-quality optical components like multi-core fibers [28]. These hardware components may reduce the computational demand but increase the sensor's overall cost. Signal processing techniques have always been used to denoise signals, and there is no exception in DAS either. Typical denoising techniques like moving average (MA) and moving differential (MD) [29], normalized differential [30], and low pass filtering (LPF) [31] can be used in DAS signals. Advanced techniques like wavelet denoising (WD) [32], and a 2D edge detection method [33] have also been explored in DAS signals for denoising. A combination of techniques using two or more methods, like an adaptive frequency wavenumber filter [34], sub-band phase shift transformation along with rotated vector sum, and optimal tracking method [32], have been used in DAS signals. Several articles also used machine learning-based approaches based on a convolutional neural network (CNN), such as the use of an iterative parallel-attention multibranch residual network (PA-MR-Net) [35], modified U-Net [36]-[37], and blind spot network (BSN) [38] in this regard.

Principal Component Analysis (PCA) is widely used for dimensionality reduction in signal processing. In the context of DAS, existing studies have primarily incorporated PCA into multi-stage or hybrid denoising frameworks rather than as a standalone solution. A. David et al. [39] demonstrated SNR improvement using PCA within a processing pipeline that includes magnitude/phase conversion and phase unwrapping; however, the study does not systematically investigate PCA component selection, parameter sensitivity, or computational complexity, which limits insight into its suitability for real-time DAS deployment. Ibrahim et al. [40] proposed an Integrated PCA (IPCA) that combines down-conversion, LMMSE filtering, and phase unwrapping to enhance ϕ-OTDR signals. Later, Wu et al. [41] introduced a wavelet decomposition method with Robust PCA (RPCA) to separate structured signals from transient noise. These techniques provide good denoising performance; however, they use numerous sequential processing stages and therefore typically require extensive parameter tuning and specific thresholding techniques tailored to the problem at hand. Additionally, the greater complexity of algorithms typically means more resources will be required to run the different processing stages, resulting in higher computational cost and greater resource requirements to implement the algorithms, and making them less attractive for real-time DAS systems.

Although PCA is widely used in signal processing, there has not yet been a comprehensive examination of its application as a standalone denoising method for DAS data. This, in turn, raises the question of whether PCA can exploit the inherent spatio-temporal correlations in DAS data with low computational complexity and minimal parameter tuning. In this article, the efficacy of a standalone PCA-based denoising framework is first examined across various strain levels with the vibration location fixed at 3 km. Its efficacy is then evaluated across different vibration locations at a fixed strain level. Finally, PCA's performance is compared with previously suggested algorithms,

namely MA, LPF, and WD. This research demonstrates that PCA alone is effective for denoising DAS signals and provides a clearer understanding of how effective and weak PCA can be across various real-world applications, enabling more informed choices about lower-complexity solutions for DAS denoising.

2. Material and methods

The research methodology adopted in this study is an experimental-analytical approach to evaluate the performance of signal denoising methods in DAS systems. Controlled laboratory experiments were undertaken to produce repeatable responses to vibration with specified sensing conditions in order to be able to systematically observe noise properties and signal behavior. The obtained data were then evaluated based on a standardized assessment system that determined the performance of denoising and makes conclusion about the appropriateness of the suggested method for the practical use of DAS.

2.1 Experimental setup

Figure 1 shows the experimental setup which includes a 100 Hz linewidth centered at 1550.12 nm, an optical modulator (MOD), two erbium-doped fiber amplifiers (EDFAs), two optical band-pass filters (BPFs), a 15 m fiber-wound piezoelectric transducer (PZT) placed between two single mode fiber (SMF) spools, a circulator, a photodetector (PD), and an oscilloscope. The continuous-wave laser output was converted into 100 ns pulses by the modulator, driven by a signal generator. These pulses were amplified by EDFA1, filtered by BPF1, and sent to the fiber under test (FUT) via a circulator. The Rayleigh backscattered light passed through EDFA2 and BPF2. It was then converted to an electrical signal by the PD and recorded by the oscilloscope at a 500 MS/s sampling rate.

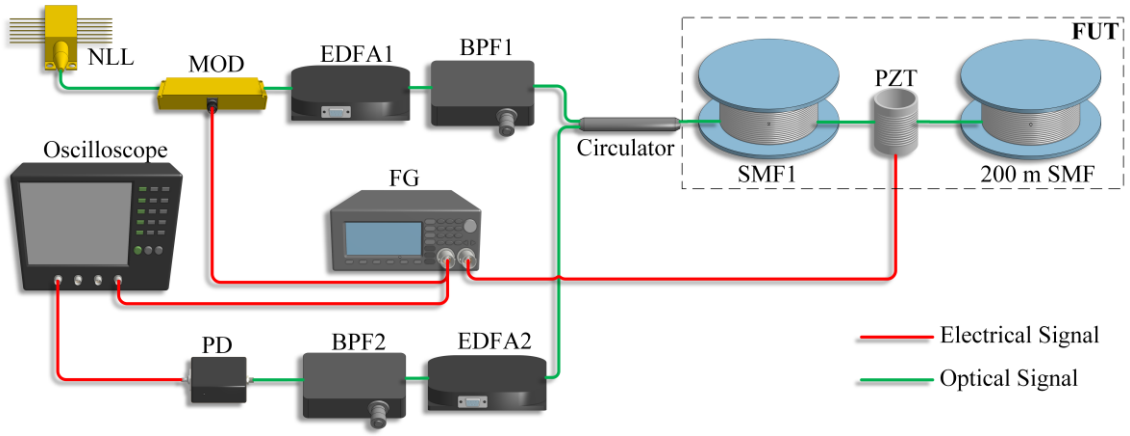

Figure 1. Experimental setup configuration

The PZT was driven by a fixed 500 Hz sinusoidal signal. For the strain-level tests, a ~3.2 km fiber spool was used as SMF1, and the PZT was driven at different voltage levels. Based on the PZT specifications, 1 V_{pp} corresponds to 41.69 nϵ. For the sensing-location tests, the SMF1 length was varied depending on available fiber spools, with the PZT voltage fixed at 2 V_{pp}. The experimental measurements were conducted in a controlled laboratory environment to minimize external disturbances. Ambient acoustic and mechanical noise sources were limited to background laboratory conditions, with no deliberate external excitation applied outside the vibration source under test. The PZT actuator was used to generate controlled vibration signals at predefined locations along the fiber. The actuator was securely coupled to the sensing fiber using mechanical clamps to ensure consistent strain transfer.

2.2 Data processing

The raw DAS data obtained from the oscilloscope can be represented as a two-dimensional array, R, as illustrated in Equation (1).

$$R_{M\times T} = \begin{bmatrix} R_{11}\, R_{12} \dots \dots \dots R_{1T} \\ R_{21}\, R_{22} \dots \dots \dots R_{2T} \\ \dots \\ \dots \\ R_{M1}\, R_{M2} \dots \dots \dots R_{MT} \end{bmatrix} \quad (1)$$

where M is the number of samples per trace, and T is the number of traces. The raw DAS data underwent several processes as shown in Figure 2. First, raw DAS signals collected through the DAS system and organized into the spatio-temporal data matrix, $R_{M,T}$. Then, standalone PCA (described in Section 2.3) is applied directly to the data matrix to suppress noise while preserving vibration-induced signal components, resulting in a denoised matrix, $D_{M,T}$. It is important to note that other denoising algorithms are applied to the same data for performance comparison, and MATLAB's *tic-toc* functions are used to calculate computational time from the beginning of denoising to the end of moving differential steps. Next, a moving differential operation is performed on all denoised data, where each trace is subtracted from its immediately preceding trace according to $\Delta D = D_{M,T+1} - D_{M,T}$, which improves vibration feature visibility [42]. Finally, the differential signals are used for vibration localization and performance evaluation through SNR and computation time analysis.

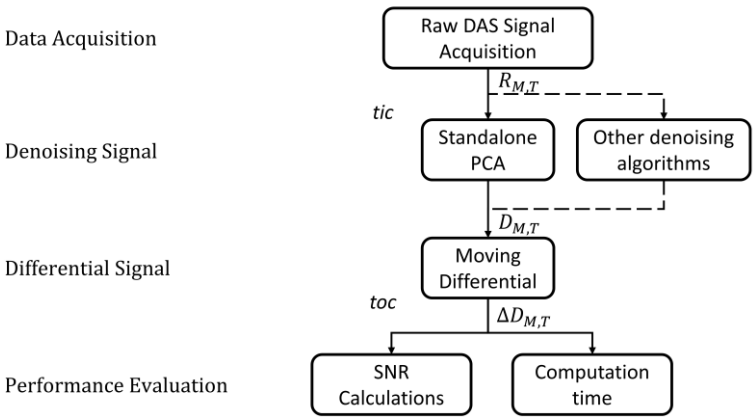

Figure 2. Overall workflow of the proposed standalone PCA DAS denoising performance evaluation study

The SNR metric was calculated from the differential traces using equation (2).

$$SNR_{dB} = 10\log\frac{P_{signal}}{P_{noise}} \quad (2)$$

where P_{signal} and P_{noise} are estimated as the variance of samples in the vibration region and non-vibration region, respectively [43]. The vibration area was defined by the region of the FUT where the PZT was placed. The entire data processing was repeated for all algorithms and parameters studied and performed using MATLAB 2024a on a 12th Gen Intel(R) Core (TM) i5-1235U 1.30 GHz CPU with 24 GB RAM. To measure computational time, MATLAB's tic and toc commands were invoked at the beginning and end of the denoising process shown in Figure 2. During data acquisition, environmental conditions, such as temperature and humidity, remained stable, with no significant fluctuations observed over the measurement period.

2.3 Denoising algorithms

This section discusses the mechanisms of PCA and briefly illustrates the other denoising techniques investigated in our experiment. The necessary equations describe their principles.

2.3.1 Principal component analysis

PCA is a dimensionality reduction technique commonly used to distinguish significant signal components from noise. Here, PCA identifies the directions (principal components) along which the signal has the highest variance, which typically aligns with the signal's actual characteristics, while the noise variance is more evenly distributed across all dimensions. In DAS, vibration-induced signals exhibit structured spatio-temporal correlation (low-rank behavior), whereas background noise is weakly correlated and spread across components. PCA leverages this contrast by concentrating signal energy into dominant components while suppressing noise-dominated components [40]. As mentioned earlier, DAS signals normally take a 2D form of $X \in R^{M \times T}$, *and* X is the data Matrix, where M is the number of samples in one trace, and T is the number of traces. X can be represented as in equation (3).

$$X = S + N \tag{3}$$

where S denotes the signal, and N denotes the noise. To apply PCA, X is first normalized to have zero means and transformed to X', and then it is decomposed using singular value decomposition to find a new basis given in equation (4).

$$X' = U\Sigma V^T \tag{4}$$

Here, U and V are orthogonal matrices of size $M \times M$ and $T \times T$, respectively, and Σ is a diagonal matrix containing singular values of size M×T representing the variance captured by each principal component. The singular values in Σ are sorted in descending order. The variance explained by each principal component I is given by the following equation 5.

$$Explained\ Variance_i = \frac{\lambda_i}{\sum_{j=1}^{N} \lambda_j} \tag{5}$$

Then, the cumulative variance was calculated by equation 6.

$$Cumulative\ Variance_i = \frac{\lambda_i}{\sum_{j=1}^{k} \lambda_j} \tag{6}$$

λ_i corresponds to the eigenvalues of the covariance matrix. Large singular values correspond to components that capture most of the signal's energy, while smaller singular values typically represent noise. From our simulations, we observed that the knee point in the cumulative variance vs. total number of components curve corresponds to more than 90% of the total variance in all cases. This graph is shown in Figure 3.

The top components were then made equal to the knee point number. A knee point detection algorithm based on the slope change of the curve was used. The denoised signal was reconstructed using equation (7).

$$X'_{denoised} = U_k \Sigma_k V_k^T \tag{7}$$

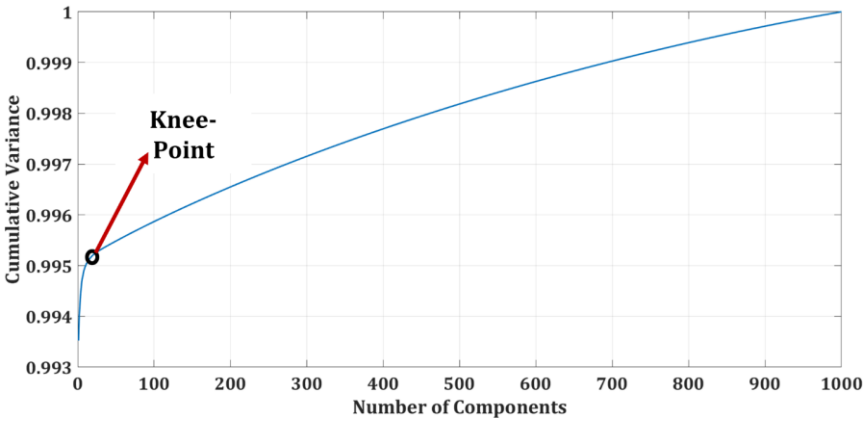

Figure 3. Cumulative variance captured by the number of components curve

where, U_k, Σ_k *and* V_k represents the matrices truncated to the top k components. The Mean of X was then added to the denoised matrix to construct the final product. In regions without external perturbation, ϕ-OTDR traces exhibit highly random fluctuations dominated by noise-like Rayleigh backscatter statistics; consequently, vibration-induced events appear as structured deviations from this background [44]. PCA transforms the data to the basis where the maximum variance in the data is found. The important components are expected to represent primary signal patterns across traces, which could correspond to significant and consistent patterns in vibration or strain along the fiber. The rest are more likely to capture random noise or small fluctuations inconsistent across traces. Because noises in DAS signals are typically uncorrelated, PCA can be beneficial for denoising them.

2.3.2 Moving average (MA)

The MA algorithm mitigates this noise by smoothing the data over a specified range, or "window size," a series of consecutive data points. Theoretically, if the sliding window length is N_w, the SNR is supposed to increase by $\sqrt{N_w}$ times, although the maximum frequency response is decreased by N_w times [29]. It is computationally simple and effective for real-time applications. For a given time series x_t and a defined window size N_w, the moving average at any point t is calculated as –

$$MA_t = \frac{1}{N}\sum_{i=0}^{N_w-1} x_{t-i} \quad (8)$$

Using equation (8), a moving average over a sliding window of N consecutive spatial samples is computed.

2.3.3 Law pass filtering (LPF)

Typically, in DAS, the perturbation signals of interest lie within a frequency range of 1 kHz but many noise components are of high frequency [45]. So, applying low-pass filtering (LPF) can enhance the signal quality of DAS by attenuating high-frequency components. However, it may introduce phase shifts and over-smoothen signals if the cutoff frequency is not chosen appropriately, potentially obscuring higher-frequency details of smaller, rapid events. Typically, an FIR filter of order n is defined by equation (9).

$$y(n) = \sum_{k=0}^{n} h(k).x(n-k) \quad (9)$$

A Finite Impulse Response (FIR) filter with an order of 50 and a cut-off frequency at 2 kHz was used for Low Pass Filtering.

2.3.4 Wavelet denoising

Wavelet Denoising (WD) decomposes signals into multiple frequency components. It aims to reduce noise across different scales (frequencies) of the DAS signal. This method is highly effective for identifying and preserving localized events. The wavelet transform decomposes the signal into wavelet coefficients at various scales and positions, representing both high- and low-frequency components. These coefficients are then analyzed to determine which represents the noise and the signal. Typically, the discrete wavelet transform (DWT) is used to split the data into approximations (low-frequency components) and details (high-frequency components). This is given by the following equation 10.

$$\begin{cases} C_A(k) = \sum_n g(2k-n).x(n) \\ C_D(k) = \sum_n h(2k-n).x(n) \end{cases} \quad (10)$$

Here, $x(n)$ is the signal, $C_A(k)$ and $C_D(k)$ are the approximation and detail coefficients, and $g(n)$ and $h(n)$ are the low-pass and high-pass filters, respectively. Noise reduction is achieved by applying a threshold to the wavelet coefficients, usually using soft or hard thresholding. Coefficients with magnitudes below a set threshold are suppressed (considered as noise), while those above the threshold are retained or modified slightly to maintain the true signal structure. The selection of the mother wavelet, decomposition level, and thresholding method will impact the denoising performance. It is found that the Daubechies 4 (db4) wavelet with 3-level decomposition and Stein's Unbiased Risk Estimate (SURE) thresholding will yield the highest value of SNR for a particular signal [46].

3. Results and discussion

PCA's denoising capability was validated using strain levels ranging from 1.2 to 10 V_{pp} vibration imposed at ~3 km from the circulator, where 1.2 V_{pp} is the minimum voltage level detectable by our DAS system. Table 1 illustrates the SNR of the DAS signal without any denoising, with PCA denoising, and the corresponding improvement. The results demonstrate that PCA improved SNR across all recorded strain levels. SNR values without denoising ranged from 4.572 dB at 1.2 V_{pp} to 13.760 dB at 10 V_{pp}. With PCA-based denoising, the SNR increased significantly, reaching 10.821 dB at the lowest strain level and 20.984 dB at the highest. The gains ranged from 4.774 dB at 8 V_{pp} to 7.223 dB at 10 V_{pp}. Improvements exceeding 6 dB at moderate strain levels of 2 to 4 V_{pp} highlight PCA's strong effectiveness across the mid-range. Even though the relative improvement decreased slightly at higher strain levels, such as 8 V_{pp}, a substantial increase was still observed. PCA successfully preserves signal characteristics while reducing noise under high-strain conditions. It improved the SNR by approximately 5 to 7 dB across all strain levels.

Table 1. SNR values without denoising and after PCA-based denoising at different strain levels, along with the corresponding SNR improvement

Strain Level (V_{pp})	Without denoising	PCA	Improvement
1.2	4.572	10.821	6.249
2	7.268	13.549	6.281
3	8.517	15.021	6.505
4	10.977	16.984	6.007
5	11.172	17.075	5.903
6	11.819	17.394	5.575
7	12.171	18.088	5.917
8	13.375	18.149	4.774
9	13.695	19.388	5.692
10	13.760	20.984	7.223

Figure 4 shows the SNR improvement provided by PCA across different vibration locations, achieved by changing SMF1 as mentioned earlier. The results show that PCA significantly improved SNR at all vibration locations. The 3 km recorded the highest gain at 6.2806 dB, followed closely by the 5 km at 6.2430 dB and the 1 km at 5.4848 dB. The 10 km showed the lowest improvement at 2.4583 dB, indicating that PCA's effectiveness decreases with increasing distance, likely due to greater noise levels and cumulative signal attenuation along longer transmission paths.

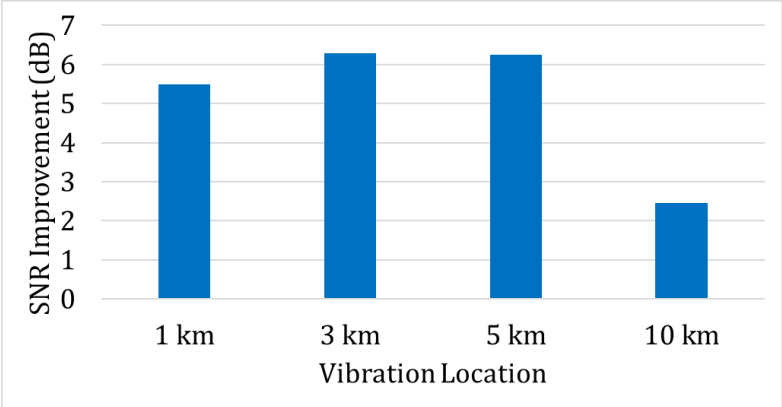

Figure 4. SNR improvements by PCA at different vibration locations. The PZT is driven by 10 V_{pp} sinusoidal wave

Figure 5 compares PCA with other proposed denoising techniques for a vibration location of 3 km. Among the evaluated algorithms, PCA achieved the highest SNR improvement, with a gain of 6.281 dB, slightly higher than LPF (6.032 dB) and well above WD (3.725 dB) and MA (1.093 dB). In terms of computational efficiency, PCA required 4.1 seconds, which, although slower than the lightweight MA approach at 0.2 seconds, was faster than LPF at 7.2 seconds and WD at 6.5 seconds. This balance of maximum noise reduction and reasonable processing time underscores PCA's effectiveness and practicality, particularly in applications where both high SNR and manageable processing time are essential.

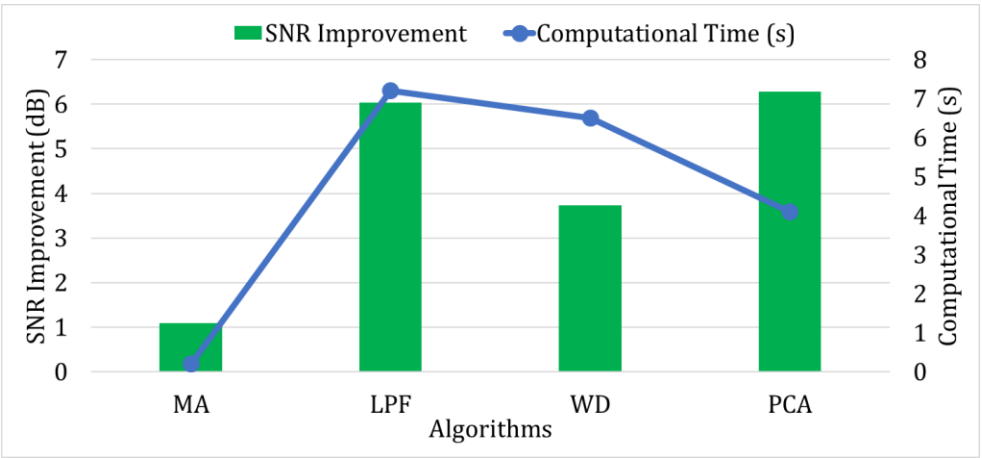

Figure 5. SNR improvement and computational time comparison of PCA and benchmark denoising techniques (MA, LPF, WD) at a fixed vibration location of ~3 km with 2 V_{pp} excitation

Figure 6 shows plotted differential signal after normalization showing effects of the different denoising algorithms performance with the raw DAS signal. Without denoising, the differential traces show large random variations along the entire fiber, indicating heavy noise. With MA, the amplitude range is slightly reduced, but a large amount of noise remains. LPF and WD remove

more noise, giving narrower amplitude ranges and smoother profiles, though some high-frequency components are still present. PCA gives the strongest noise reduction. The differential amplitudes are centered close to zero, with very little spread. The improvement is most visible in the vibration region near 3 km, where PCA removes background noise while keeping the signal intact. These plots, therefore visually confirm the SNR gains and show that PCA can achieve excellent denoising without harming signal quality.

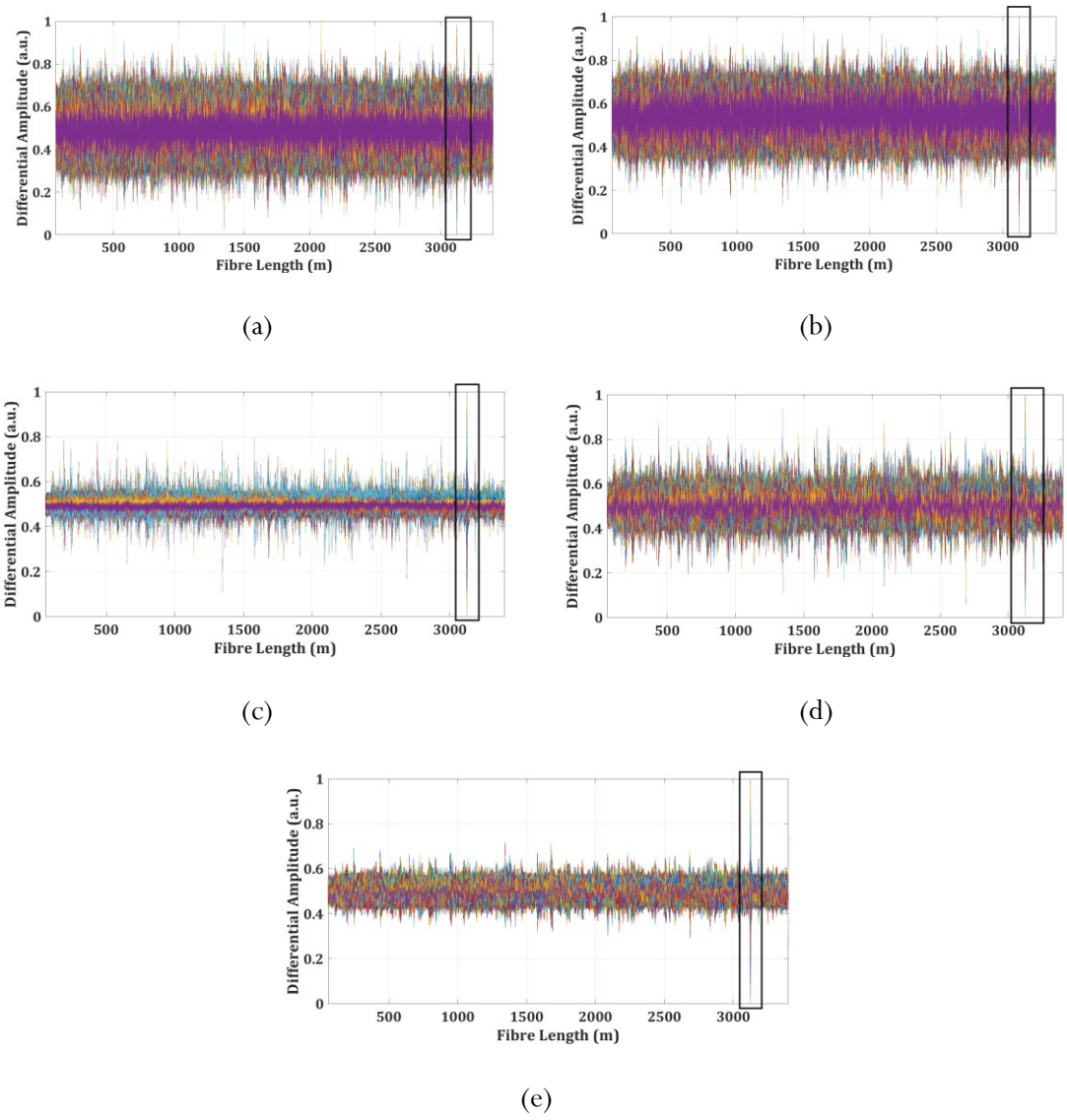

Figure 6. Differential amplitude traces of the DAS signal along the fibre length a) without denoising and after applying b) MA, c) LPF, d) WD, and e) PCA. Vibration imposed 2 V_{pp}, 500 Hz sine wave

The time–distance plots in Figure 7 give further proof of PCA's stronger denoising ability compared to MA, LPF, and WD. Without denoising, high background noise along the entire fiber hides the vibration signal at about 3 km. LPF and WD reduce the noise more than MA, making the vibration area easier to see. MA only reduces the noise slightly, leaving strong interference. PCA gives the best results, with very little background noise and a clear, sharp vibration signal. The event at 3 km is shown with excellent clarity in both time and distance, and noise is reduced across the full fiber length. These plots, hence, corroborate the earlier numerical results. They show that PCA not only improves SNR but also makes vibration events easier to see in both time and space, which is very useful for DAS.

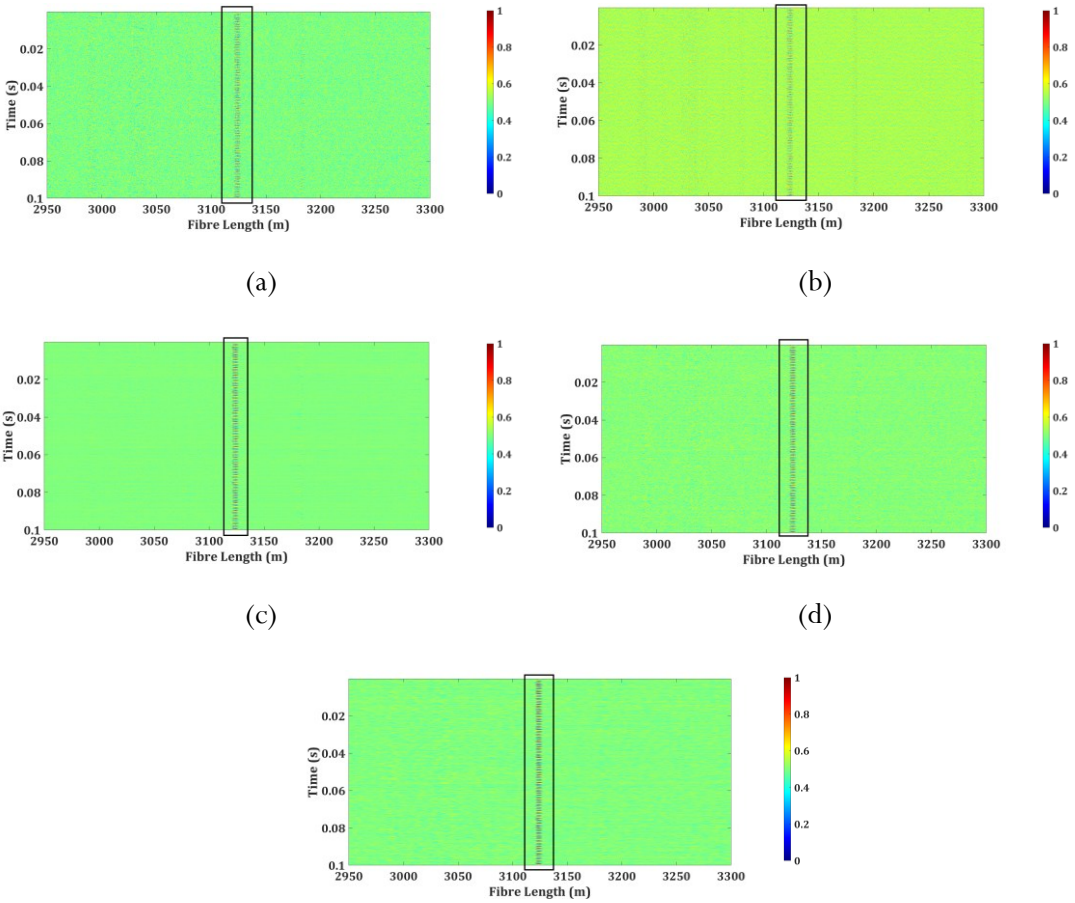

Figure 7. Time-distance plots of the DAS signal zoomed between 2.95 to 3.3 km along the fibre length a) without denoising and after applying b) MA, c) LPF, d) WD, and e) PCA. Right Panel – Color bar. Vibration imposed 2 V_{pp}, 500 Hz sine wave

The results presented in this article show that PCA is a very effective denoising method for DAS. It improved SNR across all strain levels tested (1.2-10 Vpp), with gains of 4.774-7.223 dB. The largest gains were in the moderate strain range of 2 to 4 V_{pp}, where the increase was above 6 dB. Therefore, PCA can reduce noise while preserving the signal. At higher strain levels, the gain was slightly lower, but still strong. This means PCA works well even with high input signals. Vibration location also affects performance. The highest gain was at 3 km with 6.281 dB. This was followed by 6.243 dB at 5 km and 5.485 dB at 1 km. At 10 km, the gain dropped to 2.458 dB. This drop is due to more noise and weaker signals at longer distances. The results suggest that PCA performs well at all distances but is most effective at short and medium distances. PCA also showed better SNR improvement than other methods. It beat WD by 3.725 dB and MA by 1.093 dB, by a clear margin. It also slightly beat LPF with 6.032 dB. The PCA computation time was 4.1 seconds, faster than LPF (7.2 seconds) and WD (6.5 seconds). It was slower than MA at 0.2 seconds. This balance of high noise reduction and reasonable speed makes PCA suitable for real-time or near-real-time DAS applications.

The results reported here are supported by the differential amplitude traces of the MA, LPF, WD, and PCA denoising techniques. With MA, background noise was present, but only with minimal amplitude reduction. LPF and WD produced smoother traces than the raw traces, but high-frequency noise persisted. Although PCA generated a clear representation of the vibration signal while maintaining a more compressed and zero-centered distribution of amplitude, it increased the SNR of the signal. The time–distance plots for all denoised signals showed that PCA improved SNR

and distinguished vibration events in 3D (both in time and distance) compared to LPF and WD. Background noise was eliminated from the DAS traces over the end-to-end distance, clearly highlighting the vibration signal at around 3 km. Because of PCA's demonstrated ability to reconstruct a signal with high accuracy, we believe this method would be an excellent choice for improving the sensitivity and precision of DAS when applied to denoising.

Table 2 provides a structured, side-by-side comparison of representative DAS denoising techniques reported in the literature. The comparison highlights key distinguishing factors, including algorithmic complexity, dependence on tunable parameters, and suitability for real-time implementation. This synthesis goes beyond a descriptive literature review by explicitly contrasting the proposed standalone PCA method with commonly adopted hybrid, time–frequency, and data-driven denoising strategies.

Table 2. Qualitative comparison of commonly used DAS denoising techniques based on experimentally observed behavior in this study and established characteristics reported in the literature

Ref.	Denoising method	Processing complexity	Parameter dependence	Real-Time suitability	SNR improvement (dB)	Key remarks
[37]	CNN-based	Very High	High	Moderate	N/A	Requires training data and significant computational resources
[40]	IPCA (Down-conversion + LMMSE + PCA + phase unwrapping)	High	High	Moderate	10.8	PCA is effective but embedded within a complex workflow, increasing computational burden
[41]	RPCA + Wavelet	Very High	Very High	Low	12-22	Requires careful threshold and wavelet parameter tuning
[46]	WD	Moderate	High	Moderate	Up to 15.50	Highly parameter-dependent, trial-driven.
[47]	AFDA	Moderate	Moderate	Moderate	≈3.7 (AFDA alone) Up to 10.8 (AFDA + MA-MD)	Highly parameter-dependent, trial-driven
[48]	Sequential Simple Algorithms (MA + MD + LPF)	Low	Low	High	≈3–6	Sequential simple filters, low-cost
[49]	2-D bilateral filtering	Moderate	Moderate	High	8.4-14.4	Good SNR improvement but requires window and parameter optimization

Ref.	Denoising method	Processing complexity	Parameter dependence	Real-Time suitability	SNR improvement (dB)	Key remarks
[50]	WSVD	High	Moderate	Moderate	6-7	Matrix decomposition improves SNR but involves weighting strategy and rank selection
[51]	CEEMDAN	High	High	Low	Up to 24.73	Effective for non-stationary noise but computationally intensive
[52]	ICEEMDAN–TLGMCC–WT	Very High	Very High	Low	Up to 72.18 (NRR)	Very complex, heavy tuning
This work	Stand-alone PCA	Low	Low	High	4.8–7.2	Simple, parameter-light approach exploiting spatio-temporal correlation in DAS data

Table 2 presents a comparative assessment based on both the experimental results of this work and established denoising methods. Low-pass and moving-average filtering schemes are computationally inexpensive but exhibit low adaptability and high signal distortion when applied to low-SNR DAS data, especially at high sensing distances. Wavelet denoising is more feature-preserving but is more sensitive to the choice of wavelet basis, level of decomposition and thresholding methodology which makes it difficult to apply in real-world DAS systems without significant tuning. More sophisticated, data-driven or weighted SVD-based algorithms may achieve high levels of noise suppression but come at a higher computational cost, may require extra training data, or may involve multiple steps in the process. Conversely, PCA offers a good trade-off between leveraging the natural low-rank structure of vibration responses of the DAS and moderate computational complexity and parameter insensitivity, rendering it applicable to real-time or long-range sensing operations.

According to the results, PCA, when used as a single denoising algorithm, may be effective in improving DAS signal quality without using multi-stage or hybrid signal processing pipelines. Although PCA has already been used in more sophisticated DAS signal processing models, in many cases with down-conversion, adaptive filtering, or phase unwrapping operations [39]-[41], the extent to which PCA's denoising performance is inherent to PCA on raw DAS data has not been explicitly studied. Contrary to this, the current paper separates the idea of PCA in relation to auxiliary processing steps, and demonstrates that the DAS signals induced by vibration always lie in a low-rank spatio-temporal subspace, which is directly usable in noise suppression.

At all strain levels tested, PCA produced SNR gains of about 4.8 dB to 7.2 dB, with the greatest gains occurring at intermediate levels of strain when spatio-temporal correlation between DAS traces is greatest. As argued by this trend, this observation aligns with the theoretical principle of PCA, which is based on coherent signal structure rather than on frequency-band specifications or threshold principles, and explains the better trade-off between noise reduction and signal retention, as illustrated in Table 2. Experiments over various FUT lengths also validate that PCA can still detect locations at up to about 10 km, although the performance decreases with distance as there is also attenuation of the fiber and increasing noise dominance. This effect is consistent with earlier

results from long-range DAS systems [44], [45]. Notably, despite these very adverse conditions, SNR gains can be kept, which means that PCA can still be used in a real-life situation where a long-range monitoring is required.

Table 2 summarises the results of PCA as compared to the traditional denoising methods which represent a good trade- off. Basic filtering methods like moving-average or low-pass filters have a low computational load but higher signal distortion and reduced flexibility to changing noise. Denoising algorithms using wavelets are more sensitive to feature retention but they need parameter adjustments and might not be resistant to various operating conditions [32], [41]. More complex weighted SVD or data-driven methods may provide high-quality denoising results, but tend to be more expensive to compute or rely on training data and processing pipelines [37], [50]. The suggested PCA methodology stands out as one with minimal parameter tuning, moderate computational complexity, and that works directly on raw DAS data.

What is new in this work is the controlled and systematically varied experimental data, which directly assesses PCA as an independent denoising method of DAS signals- an aspect that has not been explicitly tested in previous hybrid DAS PCA-based studies [39], [40]. Scientifically, this paper provides experimental support for the low-rank structure of DAS vibration responses over a wide strain regime and sensing distances. Technologically, the findings indicate that PCA can be a viable, simple-complexity denoising method of real-time or long-range DAS systems.

While this approach has many advantages, it is important to acknowledge its limitations. These limitations are reflected in the experimental results, particularly in the reduced SNR improvement observed at longer sensing distances and under lower signal-to-noise conditions. Lab experiments have been carried out under controlled conditions at a limited number of frequency and vibration types; however, the results indicate that real-world DAS applications may present additional challenges, where both the noise environment can be more complex and non-stationary (e.g., varying soil types), the temperature gradient can impact how DAS records data, and there may be other sources of vibration occurring at the same time. Also, PCA is a linear technique and may therefore not work well when the signal structure is highly nonlinear or when the noise distribution is strong and highly non-Gaussian. Additionally, for PCA to be effective, sufficient spatio-temporal correlation must be present, which is consistent with the stronger denoising gains observed at moderate strain levels in this study. If vibration events are distributed or have very low levels of correlation, they will likely be difficult to distinguish from noise. Finally, while PCA has relatively low computational complexity compared to some techniques, the amount of data collected through the DAS system and/or the rate of data acquisition may affect PCA's capability for ultra-long-range and ultra-high-speed DAS applications.

Thus, building on the trends observed in the experimental results, the future directions of the current work will be to verify the suggested method using DAS field data collected under a range of operational conditions, development of adaptive techniques to select dynamic principal components and evaluation of efficient preprocessing techniques, as well as the implementation of hardware-assisted methods for large-scale real-time monitoring. Also, future research can be conducted on nonlinear versions of principal component analysis, such as Kernel PCA, as well as using a data-driven deep learning-based methodology when the assumptions of linear PCA do not hold.

4. Conclusion

This article evaluates PCA performance for denoising Ø-OTDR data and compared it to other common denoising algorithms. PCA provided SNR gains from 4.774 dB to 7.223 dB across strain levels ranging from 1.2 to 10 V_{pp}. The largest gain was at 10 V_{pp}, and in the mid-range of 2 to 4 V_{pp},

the improvement was maintained above 6 dB. Hence, PCA is highly effective for improving DAS signal quality. Location-based tests showed similar results. The highest gain was at 3 km with 6.281 dB, followed by 6.243 dB at 5 km and 5.485 dB at 1 km. At 10 km, the gain dropped to 2.458 dB because of higher attenuation and noise, but the improvement was still clear. Compared with MA, LPF, and WD, PCA gave the highest SNR gain of 6.281 dB while keeping a reasonable computation time of 4.1 seconds. It was slower than MA at 0.2 seconds but faster than LPF at 7.2 seconds and WD at 6.5 seconds. Visual representations using differential traces and time–distance plots confirmed these findings. PCA removed background noise more effectively than the other methods and kept the 3- km vibration signal clear in both space and time. These results highlight PCA as a reliable and data-efficient processing tool for ϕ-OTDR DAS applications. In terms of practical considerations, the proposed standalone PCA denoising framework has strong potential for supporting real-time DAS monitoring applications due to its low computational overhead and limited reliance on user-defined parameters. In addition to this low resource requirement, the linear nature of the approach may yield inferior performance in non-linear or strongly non-Gaussian noise conditions, or in situations where vibration signals are very weak or sparsely distributed. Delivering an adaptive or non-linear version of this technique could significantly expand the applicability of this approach in future advanced research efforts.

Author's declaration

Author contribution

Monowar Mahmud: Conducted experiments and prepared the paper draft. **Aiman Ismail:** Grant receiver, interpreted and analyze data. **Fairuz Abdullah:** Supervisory role and provide advice on experimental setup. **Lee Hui Jing:** Supervisory role, reviewed and revised the manuscript. **Nur Luqman Saleh:** Advisory role on denoising algorithms and code implementation. **Abdul Hadi Sulaiman:** Advisory role on data collection.

Funding statement

This research is supported by the Malaysian Ministry of Higher Education (MOHE) FRGS grant, FRGS/1/2023/TK07/UNITEN/03/1.

Data availability

Raw data associated with this study are available. Due to its large size and the unavailability of online storage to host them, it is not possible for the authors to share the data online. Interested parties may contact the corresponding author to discuss ways to enable data sharing.

Acknowledgements

The authors are grateful to the Malaysian Ministry of Higher Education (MOHE) for the support funding as well as to UNITEN R&D Sdn Bhd and Tenaga Nasional Berhad for earlier seed funding that made the research possible (Grant #: U-TC-RD-19-04 and U-TD-RD-21-02).

Competing interest

The authors declare that they have no competing interests related to this study.

Ethical clearance

This research does not involve humans as subjects.

AI statement

ChatGPT was used to improve the language and grammar of this article. However, the contents have been comprehensively proofread by an English language expert, and the authors have cross-checked the statements for accuracy and validity.

Publisher's and Journal's note

Universitas Negeri Padang as the publisher, and Editor of Teknomekanik state that there is no conflict of interest towards this article publication.

References

[1] F. Muñoz and M. A. Soto, "Enhancing fibre-optic distributed acoustic sensing capabilities with blind near-field array signal processing," *Nat. Commun.*, vol. 13, no. 1, p. 4019, Jul. 2022, https://doi.org/10.1038/s41467-022-31681-x

[2] A. Lellouch and B. L. Biondi, "Seismic Applications of Downhole DAS," *Sensors*, vol. 21, no. 9, 2021, https://doi.org/10.3390/s21092897

[3] T. Okamoto, D. Iida, and Y. Koshikiya, "Distributed Acoustic Sensing of Seismic Wave Using Optical Frequency Domain Reflectometry," *Journal of Lightwave Technology*, vol. 41, no. 22, pp. 7036–7044, 2023, https://doi.org/10.1109/JLT.2023.3297608

[4] B. G. Gorshkov, A. E. Alekseev, M. A. Taranov, D. E. Simikin, V. T. Potapov, and D. A. Ilinskiy, "Low noise distributed acoustic sensor for seismology applications," *Appl. Opt.*, vol. 61, no. 28, p. 8308, 2022, https://doi.org/10.1364/ao.468804

[5] S. Dou *et al.*, "Distributed Acoustic Sensing for Seismic Monitoring of The Near Surface: A Traffic-Noise Interferometry Case Study," *Sci. Rep.*, vol. 7, no. 1, p. 11620, 2017, https://doi.org/10.1038/s41598-017-11986-4

[6] F. Walter *et al.*, "Distributed acoustic sensing of microseismic sources and wave propagation in glaciated terrain," *Nat. Commun.*, vol. 11, no. 1, p. 2436, 2020, https://doi.org/10.1038/s41467-020-15824-6

[7] H. Wijaya, P. Rajeev, and E. Gad, "Distributed optical fibre sensor for infrastructure monitoring: Field applications," *Optical Fiber Technology*, vol. 64, p. 102577, 2021, https://doi.org/https://doi.org/10.1016/j.yofte.2021.102577

[8] M. Jia *et al.*, "Pipeline Leaks Early Warning Based on Distributed Optical Fiber Sensing Technology," *IEEE Photonics Technology Letters*, vol. 36, no. 6, pp. 397–400, 2024, https://doi.org/10.1109/LPT.2024.3362913

[9] C. Huang, F. Peng, and K. Liu, "Pipeline Inspection Gauge Positioning System Based on Optical Fiber Distributed Acoustic Sensing," *IEEE Sens. J.*, vol. 21, no. 22, pp. 25716–25722, 2021, https://doi.org/10.1109/JSEN.2021.3116973

[10] J. Zuo *et al.*, "Pipeline Leak Detection Technology Based on Distributed Optical Fiber Acoustic Sensing System," *IEEE Access*, vol. 8, pp. 30789–30796, 2020, https://doi.org/10.1109/ACCESS.2020.2973229

[11] X. Liu, Y. Wang, B. Jin, Q. Ying, D. Wang, and Y. Wang, "Real-time distributed oil/gas pipeline security pre warning system based on Φ-OTDR," *Progress in Electromagnetics Research Symposium*, vol. 2017-Novem, pp. 1717–1719, 2017, https://doi.org/10.1109/PIERS-FALL.2017.8293412

[12] L. Ren, T. Jiang, Z. guang Jia, D. sheng Li, C. lin Yuan, and H. nan Li, "Pipeline corrosion and leakage monitoring based on the distributed optical fiber sensing technology," *Measurement (Lond).*, 2018, https://doi.org/10.1016/j.measurement.2018.03.018

[13] S. C. Huang, W. W. Lin, M. T. Tsai, and M. H. Chen, "Fiber optic in-line distributed sensor for detection and localization of the pipeline leaks," *Sens. Actuators A Phys.*, vol. 135, no. 2, pp. 570–579, 2007, https://doi.org/10.1016/j.sna.2006.10.010

[14] Y. Pan *et al.*, "Development of a distributed polarization-OTDR to measure two vibrations with the same frequency," *2015 International Conference on Optical Instruments and Technology:*

Optical Sensors and Applications, vol. 9620, p. 962002, 2015, https://doi.org/10.1117/12.2193409

[15] H. Liu, J. Ma, T. Xu, W. Yan, L. Ma, and X. Zhang, "Vehicle Detection and Classification Using Distributed Fiber Optic Acoustic Sensing," *IEEE Trans. Veh. Technol.*, vol. 69, no. 2, pp. 1363–1374, 2020, https://doi.org/10.1109/TVT.2019.2962334

[16] D. Tu, S. Xie, Z. Jiang, and M. Zhang, "Ultra long distance distributed fiber-optic system for intrusion detection," *Advanced Sensor Systems and Applications V*, vol. 8561, p. 85611W, 2012, https://doi.org/10.1117/12.2001292

[17] Y. Zhan *et al.*, "A distributed optical fiber sensor system for intrusion detection and location based on the phase-sensitive OTDR with remote pump EDFA," *Optik (Stuttg).*, vol. 225, no. May 2020, p. 165020, 2021, https://doi.org/10.1016/j.ijleo.2020.165020

[18] H. F. Taylor and C. E. Lee, "Method For Fiber Optic Intrusion Sensing. US5194847A," no. 19, 1993. https://patents.google.com/patent/US5194847A/en

[19] X. Yu, D. Zhou, B. Lu, S. Liu, and M. Pan, "Phase-sensitive optical time domain reflectometer for distributed fence-perimeter intrusion detection," *AOPC 2015: Optical Fiber Sensors and Applications*, vol. 9679, no. 50, p. 96790S, 2015, https://doi.org/10.1117/12.2199685

[20] J. C. Juarez and H. F. Taylor, "Distributed fiber optic intrusion sensor system," in *Optics InfoBase Conference Papers*, 2005, pp. 2081–2087. https://doi.org/10.1109/JLT.2005.849924

[21] X. Lu and K. Krebber, "Characterizing detection noise in phase-sensitive optical time domain reflectometry," *Opt. Express*, vol. 29, pp. 18791–18806, 2021, https://doi.org/10.1364/OE.424410

[22] K. Blotekjaer, "Fundamental noise sources that limit the ultimate resolution of fiber optic sensors," in *Optical and Fiber Optic Sensor Systems*, S. Huang, K. D. Bennett, and D. A. Jackson, Eds., SPIE, 1998, pp. 1–12. https://doi.org/10.1117/12.318192

[23] L. Zhao, X. Zhang, and Z. Xu, "A high-fidelity numerical model of coherent Φ-OTDR," *Measurement: Journal of the International Measurement Confederation*, vol. 230. 2024. https://doi.org/10.1016/j.measurement.2024.114526

[24] R. Rathod, R. Pechstedt, D. J. Webb, and D. A. Jackson, "Rayleigh backscattering in optical fibers: a noise limitation and a sensing mechanism," in *Tenth International Conference on Optical Fibre Sensors*, B. Culshaw and J. D. C. Jones, Eds., SPIE, 1994, pp. 498–501. https://doi.org/10.1117/12.184972

[25] T. Huang *et al.*, "Multiple noise reduction for distributed acoustic sensing data processing through densely connected residual convolutional networks," *J. Appl. Geophy.*, vol. 228, p. 105464, 2024, https://doi.org/10.1016/j.jappgeo.2024.105464

[26] M. Zabihi and K. Krebber, "Laser source frequency drift compensation in Φ-OTDR systems using multiple probe frequencies," *Optics Express*, vol. 30, no. 11. p. 19990, 2022. https://doi.org/10.1364/oe.460302

[27] A. Masoudi, T. Lee, M. Beresna, and G. Brambilla, "10-cm spatial resolution distributed acoustic sensor based on an ultra low-loss enhanced backscattering fiber," *Optics Continuum*, vol. 1, no. 9, pp. 2002–2010, 2022, https://doi.org/10.1364/OPTCON.468673

[28] Y. I. X. Iao *et al.*, "Fading suppression and noise reduction of a DAS system integrated multi-core fiber," vol. 32, no. 15, pp. 26793–26807, 2024, https://doi.org/10.1364/OE.528514

[29] X. Zhu, S. Zhao, X. Li, R. Zhang, and M. Kong, "Optimization of the moving averaging–moving differential algorithm for Φ-OTDR," *Appl. Opt.*, vol. 61, no. 19, p. 5633, 2022, https://doi.org/10.1364/ao.461922

[30] I. Ashry *et al.*, "Normalized differential method for improving the signal-to-noise ratio of a distributed acoustic sensor," *Appl. Opt.*, vol. 58, no. 18, p. 4933, 2019, https://doi.org/10.1364/ao.58.004933

[31] H. Wang, Y. Chen, R. Min, and Y. Chen, "Urban DAS Data Processing and Its Preliminary Application to City Traffic Monitoring," *Sensors*, vol. 22, no. 24, 2022, https://doi.org/10.3390/s22249976

[32] Z. Qin, L. Chen, and X. Bao, "Wavelet Denoising Method for Improving Detection Performance of Distributed Vibration Sensor," *IEEE Photonics Technology Letters*, vol. 24, no. 7, pp. 542–544, 2012, https://doi.org/10.1109/LPT.2011.2182643

[33] T. Zhu, X. Xiao, Q. He, and D. Diao, "Enhancement of SNR and Spatial Resolution in φ-OTDR System by Using Two-Dimensional Edge Detection Method," *Journal of Lightwave Technology*, vol. 31, no. 17, pp. 2851–2856, 2013, https://doi.org/10.1109/JLT.2013.2273553

[34] M. P. Isken, H. Vasyura-Bathke, T. Dahm, and S. Heimann, "De-noising distributed acoustic sensing data using an adaptive frequency-wavenumber filter," *Geophys. J. Int.*, vol. 231, no. 2, pp. 944–949, 2022, https://doi.org/10.1093/gji/ggac229

[35] Y. Tian, J. Sui, Y. Li, N. Wu, and D. Shao, "A Novel Iterative PA-MRNet: Multiple Noise Suppression and Weak Signals Recovery for Downhole DAS Data," *IEEE Transactions on Geoscience and Remote Sensing*, vol. 60, pp. 1–14, 2022, https://doi.org/10.1109/TGRS.2022.3170635

[36] H. Zhao, T. Bai, and Y. Chen, "Background Noise Suppression for DAS-VSP Records Using GC-AB-Unet," *IEEE Geoscience and Remote Sensing Letters*, vol. 19, pp. 1–5, 2022, https://doi.org/10.1109/LGRS.2022.3211399

[37] M. Wang, L. Deng, Y. Zhong, J. Zhang, and F. Peng, "Rapid Response DAS Denoising Method Based on Deep Learning," *Journal of Lightwave Technology*, vol. 39, no. 8, pp. 2583–2593, 2021, https://doi.org/10.1109/JLT.2021.3052651

[38] H. Ma, S. Zhou, Y. Wang, N. Wu, Y. Li, and Y. Tian, "Improving Distributed Acoustic Sensing Data Quality With Self-Supervised Learning," *IEEE Geoscience and Remote Sensing Letters,* vol. 21, pp. 1–5, 2024, https://doi.org/10.1109/LGRS.2024.3400836

[39] A. D. Atia Ibrahim, S. Lin, J. Xiong, J. Jiang, Y. Fu, and Z. Wang, "The application of PCA on Φ-OTDR sensing system for vibration detection," in 2019 18th International Conference on Optical Communications and Networks (ICOCN), IEEE, Aug. 2019, pp. 1–3. https://doi.org/10.1109/ICOCN.2019.8934672

[40] A. D. A. Ibrahim, S. Lin, J. Xiong, J. Jiang, Y. Fu, and Z. Wang, "Integrated principal component analysis denoising technique for phase-sensitive optical time domain reflectometry vibration detection," *Appl. Opt.*, vol. 59, no. 3, p. 669, 2020, https://doi.org/10.1364/ao.59.000669

[41] H. Wu *et al.*, "The Improved Wavelet Denoising Scheme Based on Robust Principal Component Analysis for Distributed Fiber Acoustic Sensor," *IEEE Sens. J.*, vol. 23, no. 19, pp. 22944–22951, 2023, https://doi.org/10.1109/JSEN.2023.3305532

[42] Y. Lu, T. Zhu, L. Chen, and X. Bao, "Distributed vibration sensor based on coherent detection of phase-OTDR," *Journal of Lightwave Technology*, vol. 28, no. 22, pp. 3243–3249, 2010, https://doi.org/10.1109/JLT.2010.2078798

[43] H. Gabai and A. Eyal, "On the sensitivity of distributed acoustic sensing," *Opt. Lett.*, vol. 41, no. 24, pp. 5648–5651, Dec. 2016, https://doi.org/10.1364/OL.41.005648

[44] A. H. Hartog, *An Introduction to Distributed Optical Fibre Sensors*, 1st ed. CRC Press, 2017. https://doi.org/10.1201/9781315119014

[45] K. E. Haavik, "On the Use of Low-Frequency Distributed Acoustic Sensing Data for In-Well Monitoring and Well Integrity: Qualitative Interpretation," *SPE Journal*, vol. 28, no. 03, pp. 1517–1532, 2023, https://doi.org/10.2118/212868-PA

[46] M. S. Yusri *et al.*, "Characterization of DWT as Denoising Method for φ-OTDR Signal," *International Journal of Nanoelectronics and Materials*, vol. 14, no. Special Issue InCAPE. pp. 333–340, 2021. https://ijneam.unimap.edu.my/images/PDF/InCAPE2021/Vol_14_SI_Dec_2021_325-332.pdf

[47] A. T. Turov, F. L. Barkov, Y. A. Konstantinov, D. A. Korobko, C. A. Lopez-Mercado, and A. A. Fotiadi, "Activation Function Dynamic Averaging as a Technique for Nonlinear 2D Data Denoising in Distributed Acoustic Sensors," *Algorithms*, vol. 16, no. 9, 2023, https://doi.org/10.3390/a16090440

[48] A. T. Turov et al., "Enhancing the Distributed Acoustic Sensors' (DAS) Performance by the Simple Noise Reduction Algorithms Sequential Application," *Algorithms*, vol. 16, no. 5, p. 217, Apr. 2023, https://doi.org/10.3390/a16050217

[49] H. He *et al.*, "SNR Enhancement in Phase-Sensitive OTDR with Adaptive 2-D Bilateral Filtering Algorithm," *IEEE Photonics J.*, vol. 9, no. 3, pp. 1–10, 2017, https://doi.org/10.1109/JPHOT.2017.2700894

[50] K. Naeem, B. H. Kim, D. J. Yoon, and I. B. Kwon, "Enhancing detection performance of the phase-sensitive otdr based distributed vibration sensor using weighted singular value decomposition," *Applied Sciences (Switzerland)*, vol. 11, no. 4, pp. 1–12, 2021, https://doi.org/10.3390/app11041928

[51] M. He, Z. Wang, and J. Qu, "Distributed Acoustic Sensor Signal Denoising Method Based On CEEMDAN-MPE," in *2022 16th IEEE International Conference on Signal Processing (ICSP)*, 2022, pp. 371–374. https://doi.org/10.1109/ICSP56322.2022.9965275

[52] G. Xiang, A. Sun, Y. Liu, and L. Gao, "Optical Fiber Technology An improved denoising method for φ -OTDR signal based on the combination of temporal local GMCC and ICEEMDAN-WT," *Optical Fiber Technology*, vol. 87, no. September, p. 103949, 2024, https://doi.org/10.1016/j.yofte.2024.103949

Nomenclature

Symbol	Meaning	Unit
Σ	Diagonal matrix of singular values	–
λ_i	Eigenvalue corresponding to the ith principal component	–
$C_A(k)$	Approximation coefficients in Discrete Wavelet Transform	–
$C_D(k)$	Detail coefficients in Discrete Wavelet Transform	–
ΔD	Moving differential between consecutive traces	–
f_c	Cut-off frequency of Low Pass Filter	Hz
g(n)	Low-pass filter coefficients in Wavelet Transform	–
h(n)	High-pass filter coefficients in Wavelet Transform	–
k	Number of retained principal components	–
M	Number of samples per trace	–
MA_t	Moving average of N samples	–
n	Filter order	–
N	Noise Component	–
N_w	Window size for moving average	–
P_{signal}	Signal Power	dB
P_{noise}	Noise Power	dB
R	Raw DAS data array	–
S	Signal Component	–
T	Number of traces	–
U, V	Orthogonal matrices from Singular Value Decomposition	–
U_k, Σ_k and V_k	Truncated $U, \sum$ and V	–
x_t	Signal value at sample t	–
X	Original DAS Matrix	–
X′	Mean-centered DAS matrix	–